Article type : Original Article

Potential Roles of YCF54 and Ferredoxin-NADPH Reductase for Magnesium Protoporphyrin Monomethylester Cyclase

Josephine Herbst[1], Annabel Girke[1], Mohammad Reza Hajirezaei[2], Guy Hanke[3], Bernhard Grimm[1]

[1] Humboldt-University Berlin, Life Sciences Faulty, Institute of Biology/Plant Physiology, Philippstraße 13, Building 12, 10115 Berlin

[2] Leibniz Institute of Plant Genetics and Crop Plant Research (IPK), Molecular Plant Nutrition, OT Gatersleben, Corrensstrasse 3, D-06466 Seeland

[3] Department of Cell and Molecular Biology, Fogg Building Queen Mary University of London Mile End Road London E1 4NS UK

Corresponding author: bernhard.grimm@rz.hu-berlin.de

Running head: YCF54 and FNR in chlorophyll synthesis

Keywords: tetrapyrrole biosynthesis, chlorophyll synthesis, photosynthesis, electron transfer, NADPH, protein-protein-interaction

Abbreviations:

ACSF, AEROBIC CYCLYSATION SYSTEM Fe-CONTAINING SUBUNIT; ALA, 5-aminolevulinic acid; AS, antisense lines; BchE, anaerobic MgProtoME cyclase; BiFC, Bimolecular fluorescence complementation; blue-native polyacrylamide gel electrophoresis, BN-PAGE; CAO, Chl *a* oxygenase; Chl, chlorophyll; CHLG, Chl synthase; Chlide, chlorophyllide; CHLM, MgProto methyltransferase; CHLP, geranylgeranyl; COS, co-suppression; DVR, divinyl reductase; FLU, FLUORESCENT; Fd,

ferredoxin; FNR, Fd:NADP(H)-oxidoreductase; GluTR, glutamyl-tRNA reductase; LCAA, LOW CHLOROPHYLL ACCUMULATION A; LHC, light-harvesting complex; LHCPs, light-harvesting Chl-binding proteins; LIL3.1, light-harvesting like protein 3.1; MgProto, Mg protoporphyrin; MgProtoME, MgProto monomethylester; NDH, NADH dehydrogenase; NTRC, NADPH-dependent thioredoxin reductase; OEX, over-expression; Pchlide, protochlorophyllide; POR, light-dependent Pchlide oxidoreductase; Proto, protoporphyrin IX; PSI, photosystem I; PSII, photosystem II; S, sense lines; TBS, tetrapyrrole biosynthesis; ycf54, hypothetical chloroplast open reading frame 54 (ycf54)

Abstract

Chlorophyll is synthesized from activated glutamate in the tetrapyrrole biosynthesis pathway through at least 20 different enzymatic reactions. Among these, the MgProto monomethylester (MgProtoME) cyclase catalyzes the formation of a fifth isocyclic ring to tetrapyrroles to form protochlorophyllide. The enzyme consists of two proteins. The CHL27 protein is proposed to be the catalytic component, while LCAA/YCF54 likely acts as a scaffolding factor. In comparison to other reactions of chlorophyll biosynthesis, this enzymatic step lacks clear elucidation and it is hardly understood, how electrons are delivered for the NADPH-dependent cyclization reaction. The present study intends to more precisely elucidate the role of LCAA/YCF54. Transgenic Arabidopsis lines with inactivated and overexpressed *YCF54* reveal the mutual stability of YCF54 and CHL27. Among the YCF54-interacting proteins, the plastidal ferredoxin-NADPH reductase (FNR) was identified. We showed in *N. tabacum* and *A. thaliana* that a deficit of FNR1 or YCF54 caused MgProtoME accumulation, the substrate of the cyclase, and destabilization of the cyclase subunits. It is proposed that FNR serves as a potential donor for electrons required in the cyclase reaction and connects chlorophyll synthesis with photosynthetic activity.

Introduction

The plant tetrapyrroles chlorophyll (Chl), heme, siroheme and phytochromobiline are required in multiple cellular processes, such as light absorption, energy transduction in photosynthesis and respiration, light signaling and nitrogen and sulphur assimilation, which makes them indispensable for life on Earth. Tetrapyrroles are formed from 5-aminolevulinic acid (ALA), which is the first committed precursor of tetrapyrrole biosynthesis (TBS) (Tanaka and Tanaka, 2007). Always eight molecules of ALA participate in the synthesis of

protoporphyrin IX (Proto), which is the substrate of both Mg chelatase and Fe chelatase. At this metabolic branch point either Mg protoporphyrin (MgProto) or protoheme are formed, which are channeled into either the Chl-synthesizing Mg branch or the heme and bilin-synthesizing Fe branch, respectively (Tanaka *et al.*, 2010, Tanaka and Tanaka, 2011, Brzezowski *et al.*, 2015). For Chl synthesis, MgProto methyltransferase (CHLM) converts MgProto into MgProto monomethylester (MgProtoME) by esterification of the propionate side chain at C13 with a methyl group. In a subsequent reaction step, MgProtoME is converted into protochlorophyllide (Pchlide), before the light-dependent Pchlide oxidoreductase (POR), divinyl reductase (DVR) and Chl synthase (CHLG) complete the synthesis of Chl *a*. Finally, Chl *a* oxygenase (CAO) converts Chl *a* to Chl *b* (Tanaka and Tanaka, 2007).

MgProtoME is the substrate of the MgProtoME cyclase, which catalyzes the formation of a fifth isocyclic ring from the 13-methyl propionate. This complex reaction is performed by two different enzymes depending on whether conditions are anaerobic or aerobic. The anaerobic bacterial MgProtoME cyclase (BchE) utilizes water as the source of oxygen (Porra *et al.*, 1996, Porra *et al.*, 1998). The oxygen-dependent cyclase, AEROBIC CYCLYSATION SYSTEM Fe-CONTAINING SUBUNIT (ACSF), is present in different groups of photosynthetic organisms and requires molecular oxygen and NADPH for catalysis (Pinta *et al.*, 2002, Ouchane *et al.*, 2004). In oxygenic Chl-forming organisms, ACSF homologs have been reported to contribute to the cyclization reaction: CRD1 and CTH1 in *Chlamydomonas reinhardtii,* (Moseley *et al.*, 2002), XANTHA-L in barley (Rzeznicka *et al.*, 2005), the cycI/II/chlA1/2 proteins in *Synechocystis sp. PCC 6803* (Minamizaki *et al.*, 2008, Peter *et al.*, 2009) and CHL27 in *Arabidopsis thaliana* (Tottey *et al.*, 2003).

The ACSF protein belongs to the family of di-iron carboxylate proteins, which contain a di-iron-binding motif including glutamate and histidine residues (Nordlund and Eklund, 1995). In a similar mechanism to that of monooxygenases, dioxygen-dependent oxidation-hydroxylation reactions are catalyzed within the di-iron cluster. The complex reaction of isocyclic ring formation requires an initial donation of electrons for the reduction of the di-iron cluster cofactor, but ultimately releases six electrons (oxidation) during catalysis and is proposed to consist of three sequential steps: 1. Hydroxylation of the methylpropionate at the C ring, 2. oxidation of the hydroxyl group to a carbonyl and 3. ligation of the α-carbon of

MgProto 6-methyl-β-ketopropionate to the 7-meso bridge carbon between the C and D pyrrole rings of the porphyrin to form divinyl Pchlide (Hollingshead *et al.*, 2012).

Despite a general understanding of the cyclization mechanism, the structural and molecular requirements for the catalytic conversion of MgProtoME to Pchlide still remain unclear, leaving the cyclase reaction among the poorest understood steps of TBS. Several subunits are thought to be necessary for the oxygen-dependent cyclisation reaction to provide cofactors, donate electrons, bind the substrate and deal with several metabolic intermediates formed during catalysis (Walker *et al.*, 1991). The cyclase complex was proposed to consist of at least three components: a di-iron hydroxylase, a subunit for electron transfer (supply of reducing power) and a scaffold protein (Wong and Castelfranco, 1984, Walker *et al.*, 1991, Berthold and Stenmark, 2003). In *Cucumis sativus L.* the combined soluble and membrane-bound fraction of isolated chloroplasts is required to obtain cyclase activity, suggesting that components of the cyclase complex are located in the membrane and stroma, respectively (Wong and Castelfranco, 1984, Rzeznicka *et al.*, 2005).

Besides the ACSF homolog, a second protein was recently identified, which supports the cyclase activity and was designated hypothetical chloroplast open reading frame 54 (Ycf54) in *Synechocystis PCC 6803* (Hollingshead *et al.*, 2012) and LOW CHLOROPHYLL ACCUMULATION A (LCAA) in tobacco, respectively (Albus *et al.*, 2012). While the precise role of ycf54/LCAA remains unclear, it was considered to play an important structural role in the cyclase as a potential scaffold protein (Albus *et al.*, 2012, Bollivar *et al.*, 2014). In addition, it is suggested that ycf54/LCAA connects the cyclase reaction with the adjacent steps of TBS (Albus *et al.*, 2012).

Apart from molecular oxygen, the cyclisation depends on reduction of ferric ions in the catalytic subunit of the cyclase (Walker *et al.*, 1991, Bollivar and Beale, 1995). Continuing research on the structure and function of the cyclase underlined the need for additional reductases to regenerate NADPH. Different reducing mechanisms have been suggested. The NADPH-dependent thioredoxin reductase (NTRC) was shown to prompt protection of the cyclase activity (Stenbaek *et al.*, 2008), although it was proposed that NTRC primarily function to remove free radicals rather than to directly donate electrons to the reaction. The photosynthetic plastoquinol pool was suggested to be a reductant for the cyclase di-

iron cluster (Steccanella *et al.*, 2015). The authors reported that quinols could potentially donate electrons to the cyclase reaction and thus connect Chl synthesis with the redox state of the photosynthetic thylakoid membrane.

Alternative sources of photosynthetic electrons generated at photosystem I (PSI) include ferredoxin (Fd), which is the first acceptor and donates electrons to multiple redox enzymes, including Chl *a* oxygenase (CAO, Tanaka *et al*., 1998). The majority of these electrons are utilized by Fd:NADP(H)-oxidoreductase (FNR) to generate NADPH. Higher plants possess several gene copies for the plastid-localized FNR (Hanke *et al.*, 2005), which is also capable of the reverse reaction, using heterotrophically derived NADPH to support Fd-dependent metabolism in the dark. As examined for MgProtoME cyclase, FNR isoforms are present in both soluble and membrane compartments, and this trait is preserved from cyanobacteria (Thomas *et al.*, 2006) through to higher plants (Hanke *et al.*, 2005, Okutani *et al.*, 2005). Single Arabidopsis *fnr* knock-out mutants are viable, although they show variation in the amount of FNR recruited to the membrane (Lintala *et al.*, 2009), while the double mutants are lethal (Lintala *et al.*, 2012).

The physiological significance of differential FNR allocation in stroma and membrane fractions for energy distribution was underlined in chloroplasts (Hanke *et al.*, 2008). In Arabidopsis, FNR1 is the most abundant isoform at the membrane and required for membrane–binding of FNR2 (Hanke *et al.*, 2005, Lintala *et al.*, 2009). FNR is tethered to the thylakoid membrane by specific binding proteins (Benz et al., 2009; Juric et al., 2009) and several FNR-interacting complexes have also been described, including PSI (Anderson *et al.*, 1992), NADH dehydrogenase (NDH) (Guedeney *et al.*, 1996) and cytochrome b6f (Clark *et al.*, 1984, Zhang *et al.*, 2001). These studies emphasize the role of FNR in both linear and cyclic photosynthetic electron transport (Joliot and Johnson, 2011) and the functional diversity of FNR isoforms is also reflected in their differential distribution between these different subchloroplastic locations.

In the present study we further investigated the function of YCF54 in higher plant Chl synthesis and searched for potential interacting proteins. YCF54 was overexpressed and analyzed in *A. thaliana* seedlings. Interestingly, FNR1 was identified as an interacting protein

of YCF54 and CHL27. Our results support a model in which FNR is involved in electron supply to the MgProtoME cyclase reaction.

Results

Loss of YCF54 protein is accompanied with leaf chlorosis and decreased CHL27 accumulation

Transformation of *A. thaliana* wild-type plants with the pXCS-HA-Strep vector carrying the 35S::YCF54-HA-Strep gene construct resulted in transgenic lines with two different phenotypes (Figure 1A). We identified either transgenic lines with pale green leaves or wild type-like leaf pigmentation (Figure 1A). The green transformants are characterized by a strong accumulation of the YCF54-HA-Strep protein, whereas the reduced Chl content of pale green seedlings correlated with reduced YCF54 content (Figure 1B/D). Because of the phenotype and the corresponding accumulation of YCF54, we termed the selected transformants either co-suppression lines (YCF54-COS) or over-expression (YCF54-OEX) lines. The loss of YCF54 protein was observed in the representative YCF54-COS lines in comparison to wild-type (Col-0), although two-times more total *YCF54* transcript accumulated (Figure 1C), but only very low content of endogenous RNA. It was not clarified whether co-suppression was due to compromised translation or enhanced YCF54 degradation. OEX lines accumulated up to three orders of magnitude more transgenic *YCF54* mRNA relative to wild type and the endogenous RNA content remained stable (Figure 1C).

In comparison to wild type, immunoblot analysis revealed that CHL27 content increased in response to YCF54 accumulation in the OEX lines, while low YCF54 content of the transgenic COS lines correlated with decreased CHL27 abundance (Figure 1B). The *CHL27* transcript levels were slightly elevated in YCF54-COS lines and remained at wild-type levels in OEX lines (Figure 1C). These findings are explained by either elevated stability of CHL27 in the presence of excess YCF54 or decreased stability of CHL27 as result of missing YCF54.

YCF54 deficiency impairs the cyclase reaction and excess YCF54 correlates with increased ALA synthesis

It is proposed that YCF54 is required for the MgProtoME cyclase reaction. The steady state levels of substrate and product of the cyclization reaction were analyzed in the selected transgenic YCF54-expressing lines. Elevated MgProtoME and decreased Pchlide and chlorophyllide (Chlide) levels were observed in the YCF54-COS lines (Figure 2A-C), which correlated with lower Chl content and an enhanced Chl a/b ratio (Figure 1D/E). The YCF54-OEX lines also contained wild-type-like MgProto and MgProtoME contents, while Pchlide content was elevated compared to the control. We examined further whether modified YCF54 content also affected ALA synthesis. We hypothesized that ALA synthesis is modulated by feedback control through the late enzymatic steps of Chl synthesis, as it was reported for transgenic lines with modified Mg chelatase, CHLM activity and Chl synthase (Papenbrock *et al.*, 2000, Alawady and Grimm, 2005, Shalygo *et al*., 2009). The YCF54-COS lines showed decreased ALA synthesis capacity, which is consistent with their lower Chl content (Figure 1D). Oppositely, YCF54-OEX lines demonstrated an increased ALA synthesis rate (Figure 2D), which correlates with an enhanced metabolic flow through the pathway. In summary, these results indicate that balanced YCF54 content is a requirement for adequate cyclase activity, with feedback-control on ALA biosynthesis rate and the supply of tetrapyrrole intermediates to the pathway.

YCF54 deficiency leads to massive loss of photosynthetic protein complexes

The lower Chl content in the COS lines correlated with a predominantly stronger decrease in Chl b content than Chl a (Figure 1E) and, at first view, suggests a preferential loss of the antenna complexes relative to the core proteins of the two PSs. Immunoblot analysis confirmed a decrease in light-harvesting Chl-binding proteins (LHCPs) of both photosystems in YCF54-COS lines (Figure 3A), however LHCA1 content tends to be more diminished than LHCB1. The YCF54-OEX lines accumulate wild-type-like amounts of LHCA and LHCB. The COS lines showed also a reduced PsbA (D1) and PsaD content, at which PsbA content of the YCF54-COS lines was stronger decreased than in control and YCF54-OEC lines (Figure 3A)

In comparison to an *A. thaliana chl27* knockdown line and wild type, we examined the accumulation of pigment-protein complexes in the thylakoid membranes of a representative YCF54-COS line. Separation of solubilized protein complexes from thylakoid membranes by blue-native gel electrophoresis (BN-PAGE) revealed the loss of the different PSII-LHCII supercomplexes as well as the LHC assembly complex, LHCII trimers and monomers in response to impaired expression of YCF54 and CHL27 (Figure 3B). The results generally highlighted a stronger negative effect on the content of photosynthetic complexes in the YCF54-COS line than in *chl27.* Comparing the loss of photosynthetic protein complexes of the YCF54-COS line and *chl27,* it is remarkable that the PSII-LHCII complex C2S2 and the LHCII assembly complexes were more significantly diminished in YCF54-deficient plants. Measuring the emission of 77K Chl fluorescence revealed a drastic decline of the emission peak at 730 nm (Figure 3C) relative to the normalized 680 nm emission peak. These data reflect a strong impairment of PSI in response to lower cyclase subunit contents.

Search for YCF54-6xHis interacting proteins

Arabidopsis YCF54 and CHL27 were reported to be vital for the cyclization reaction (Albus *et al.*, 2012, Hollingshead *et al.*, 2012). However, it still remains an open question, how electrons are donated to the cyclase reaction and whether YCF54 acts only in the cyclase complex or has additional roles in chloroplast biogenesis. We searched for YCF54 interaction partners by performing pull-down assays using recombinant His-tagged YCF54 as bait. We initially expected that proteins involved in the late steps of TBS would essentially be connected with YCF54. In addition, the oxygenic cyclase resembles monooxygenase-related proteins (Berthold and Stenmark, 2003). Besides the CHL27 subunit and YCF54, the monooxygenase-type complexes include an additional reducing subunit. We initially performed immunoblot analysis with the eluates by using available antibodies against proteins which are closely related to catalytic Pchlide conversion: CHL27, the three POR variants, and geranylgeranyl reductase (CHLP), which provides the alkyl chain for Chl biosynthesis. Apart from the confirmed detection of interaction partner CHL27 (Figure 4A), no other Chl synthesis protein could be detected by immunoblotting.

One of the potential candidates for electron transfer to NADPH is plastid-localized ferredoxin-NADP(H) oxidoreductase 1 (FNR1). Using an anti-FNR antibody an immune-reacting band was obtained from the eluate of the pull-down assay (Figure 4A). FNR1 is a leaf-type-specific FNR-isoform (Hanke *et al.*, 2005). A control experiment, using only chloroplast extracts and the empty Ni-NTA matrix revealed no immune-reacting bands neither CHL27 nor FNR1.

Bimolecular fluorescence complementation (BiFC) assays were performed to verify the novel interaction between YCF54 and FNR1. The BiFC assay confirmed in-vivo interaction between each of the two cyclase subunits CHL27 and YCF54 and FNR1 (Figure 4B).

FNR1 **deficiency causes altered TBS**

FNR1 has previously been described as a branch point in chloroplast metabolism, capable of altering electron partitioning depending on its location (Hanke *et al.*, 2008, Korn *et al.*, 2009, Joliot and Johnson, 2011, Twachtmann *et al.*, 2012, Alcantara-Sanchez *et al.*, 2017)). To investigate the new role for FNR in partitioning electrons to the reducing steps of the cyclase reaction, we examined the cyclase reaction in plants with altered FNR content. Firstly, we compared TBS in *A. thaliana* YCF54-COS-lines with *fnr1* (SALK line 085403), a knockdown mutant of FNR1 (Lintala *et al.*, 2007, Hanke *et al.*, 2008) by examining the abundance of cyclase subunits and contents of the cyclase substrate and product. The *fnr1* mutant accumulated less YCF54, similar to the YCF54-COS lines, but had wild-type levels of CHL27 (Figure 5A). Interestingly, *fnr1* also accumulated more MgProtoME than the control line, although the MgProtoME levels were not as much enriched as in the YCF54-COS lines (Figure 5C). While the COS line contained decreased Pchlide and Chlide contents as a direct result of impaired cyclase reaction, Pchlide slightly accumulated in *fnr1* in comparison to control (Figure 5D/E). The modified accumulation of tetrapyrrole intermediates supports a direct role for FNR in TBS rather than a general downregulation of Chl synthesis associated with impaired photosynthesis. Thus, these results argue for perturbed cyclase reaction upon FNR1 deficiency. It is also noteworthy that in a reciprocal analysis, FNR1 accumulated in *A. thaliana* YCF54-OEX lines to higher amounts, while the YCF54-COS lines were characterized by lower FNR1 levels (Figure 5B).

To verify the potential impact of FNR on the cyclase reaction in other plant species, we also examined representative *FNR1*-antisense (AS) (Rodriguez *et al.*, 2007) and sense (S) lines from tobacco (*Nicotiana tabacum*) for any impact on the MgProtoME cyclase reaction. FNR-AS lines with a strong decrease in green pigmentation were characterized by yellow-green young leaves (Figure 6A/C). The FNR-S lines contained wild-type Chl content. We used three selected FNR1-AS lines, which were characterized by gradually decreased FNR content and two FNR-S lines, which over-accumulated FNR in comparison to control plants. FNR1-AS lines contained lower CHL27 amounts, but similar YCF54 levels in comparison to control (Figure 6B). In contrast, the FNR1-S lines contained more CHL27 and YCF54 in comparison to control. It is therefore suggested that FNR levels impact on the MgProtoME cyclase reaction and correlate with the stability of the CHL27 subunit.

Compared to tobacco wild-type, the FNR1-AS line accumulated detectable levels of MgProto and up to 3-fold more MgProtoME (Figure 6D). The MgProto and MgProtoME contents of the FNR1-S line more closely resembled those of control plants. Surprisingly, the FNR1-AS line also accumulated more Pchlide than wild-type seedling, while the FNR1-S line contained less Pchlide than both control and antisense lines (Figure 6E). Thus, disturbed MgProtoME levels and cyclase activity in both Arabidopsis and tobacco plants in response to altered FNR contents confirmed the negative impact of FNR deficiency on the cyclase reaction and a positive impact of excess FNR on Chl27 and YCF54/LCAA accumulation.

The steady state contents of tetrapyrrole intermediates differed between tobacco leaves and Arabidopsis seedlings (Figures 2 and 6), presumably because their relative growth rates resulted in variable metabolic fluxes through TBS. Bearing such differences in mind, the impact of decreased FNR activity on the cyclase reaction is similar between Arabidopsis and tobacco and strongly supports a functional link between FNR and MgProtoME cyclase. Considering the elevated Pchlide levels in both plant species despite the decreased FNR accumulation, an additional negative impact of decreased FNR levels on the NADPH-requiring Pchlide reduction of POR cannot be excluded.

Discussion

Arabidopsis YCF54 deficiency impacts the stability of the cyclase protein CHL27 and photosynthetic protein complexes

The Mg branch of TBS generates the essential metabolic intermediates for Chl formation. Impaired synthesis of precursors decreases the supply of Chl and, consequently, perturbs assembly of the photosynthetic complexes (Figure 3). The formation of pale green leaves was the first obvious macroscopic phenotype of Arabidopsis seedlings with YCF54 deficiency due to inadequate Chl content (Figure 1A/D). The same observation was previously reported in response to LCAA deficiency, the YCF54 homolog in *N. tabacum* (Albus *et al.*, 2012). Immunological analysis of the transgenic lines with *YCF54* inactivation or overexpression underlined the mutually stabilizing effect of YCF54 on CHL27 (Figure 1B)., as it has been previously shown for Ycf54/LCAA deficient tobacco and *Synechocystis PCC6803* (Albus *et al.*, 2012, Hollingshead *et al.*, 2012, Hollingshead *et al.*, 2017).

As result of the interdependent stability of both proteins, the cyclase reaction was impaired in the Arabidopsis YCF54-COS lines, which was demonstrated by the accumulation of MgProtoME and lower Pchlide content in comparison to wild type (Figure 2A/B). Due to the impaired cyclase reaction, less Chl accumulated, the Chl a/b ratio was elevated and the content of photosynthetic protein complexes diminished (Figure 3B). Severely decreased contents of the PSII-LHCII supercomplexes with different numbers of LHCII trimers but also the LHC assembly complex and LHC trimers characterized the photosynthetic complexes in BN-gels. However, immunological sample analysis for candidate proteins from antenna and core complexes of both PSs indicate that the content of LHCPs and core proteins of PSI are more decreased than those of PSII. The 77K Chl fluorescence emission spectra revealed a stronger decrease in PSI-LHCI complexes relative to the PSII-LHCII complexes, which would be in line with the immunoblot results (Figure 3A/C). It is not yet clear, whether the deregulated PSI/PSII ratio is due to phototoxicity of accumulating Mg-porphyrins or lower Chl content. Additional regulation of the PSI to PSII ratios cannot be entirely excluded to contribute to the disproportional decrease in core PSI chlorophyll fluorescence and could be a compensatory response to the disproportionate loss of PSII antenna and decreasing PSII efficiency.

Our analyses are similar to previous observations of severely decreased PSI-complexes in response to deficient CRD1 and CHL27 in *C. reinhardtii* and *A. thaliana,* respectively (Moseley *et al.*, 2002, Tottey *et al.*, 2003). It remains an open question as to how the cyclase reaction is connected to the active PSI complex. As decreased activity of neither enzyme adjacent to the cyclase in the pathway (neither CHLM, Mg chelatase nor POR) results in interdependency with PSI activity and stability, the potential interaction between PSI and the cyclase reaction will be a target for future research.

The role of YCF54 in tetrapyrrole biosynthesis

YCF54/LCAA has been described as a potential accessory and scaffolding protein (Albus *et al.*, 2012, Hollingshead *et al.,* 2012). Experimental evidence suggested that lowering levels of YCF54 lead to decreased contents of other TBS enzymes from Proto to Chlide (Peter *et al.*, 2009, Bollivar *et al.*, 2014). Apart from CHL27, additional YCF54 interaction partners of TBS were not identified.

Hollingshead *et al.* (2016) identified a set of interaction partners of the cyanobacterial Ycf54, including POR, DVR and CHLP. In Arabidopsis, POR and CHLP interact with the LHC-like 3 protein (LIL3), a member of the LHC protein family (Hey et al., 2017). LIL3 was proposed to direct the catalytic products to the subsequent enzyme Chl synthase and to organize the later steps of Chl synthesis prior to assembly of Chl into the photosynthetic complexes (Tanaka *et al.*, 2010). As LIL3 is not found in cyanobacteria, a supportive role of Ycf54 in the assembly and organisation of the cyanobacterial Chl synthesis besides scaffolding for the cyclase reaction is not excluded.

Mass spectrometry analysis after BN PAGE of solubilized protein complexes of thylakoid membranes revealed comigration of CHL27 with PORB, PORC, FLU (a negative regulator of ALA biosynthesis) and CHLP (Kauss *et al.*, 2012). This protein assembly was accompanied by glutamyl-tRNA reductase (GluTR, the initial and rate limiting TBS enzyme) in darkness (Kauss *et al.*, 2012). Future studies have to verify to which extent these potential assembly complexes in Chl metabolism contain also YCF54 as an additional factor and contribute to the distinction between light-dependent Chl synthesis and dark-dependent inactivation of the pathway.

YCF54 and FNR1 are potential interacting partners

As NADPH donates electrons to the cyclase reaction, an associated NADPH-regenerating mechanism has been previously proposed (Walker *et al.*, 1991; Stenbaek *et al.*, 2008, Steccanella *et al.*, 2015). Purification strategies using chloroplast or cyanobacterial protein fractions were previously undertaken to define both soluble and membrane protein components required for the reconstitution of the cyclization reaction (Walker *et al.*, 1991), but a reducing subunit or a reductase were definitively not assigned to the aerobic cyclase reaction. Using the bait protein YCF54 the leaf type FNR1 was identified as a new interaction partner from chloroplast extracts (Figure 4). Based on this we hypothesized that FNR1 could contribute to the reducing step by donation of electrons for cyclase-bound NADPH.

Using the pull-down assay as an initial screen for potential interaction partners, the structural and functional interaction between FNR1 and the cyclase reactions was confirmed by conducting a BiFC assay and analysing transgenic lines and mutants with deregulated FNR1 expression. Tobacco FNR1-S and AS plants were compared with wild type (SNN) and Arabidopsis *fnr1* with YCF54-OEX and COS lines. These Arabidopsis and tobacco mutants with FNR deficiency or over-production showed modified content of YCF54 and CHL27. In previous studies a strong decline in NADPH/$NADP^+$ ratios was demonstrated as result of the *FNR1* silencing, which further leads to a downregulation of the photosynthetic machinery in response to the over-reduction of PSI (Hajirezaei *et al.*, 2002, Lintala *et al.*, 2012). Interestingly, although FNR1 is proportionally more membrane-bound than FNR2 in Arabidopsis (Hanke *et al.*, 2005), and knock-out of the *FNR* gene resulted in decreased chlorophyll content and loss of membrane-binding by the alternative, FNR2 isoform (Lintala *et al.*, 2007, Hanke *et al.*, 2008), no evidence has previously been presented for FNR1 involvement in TBS.

Given the redox stoichiometry of the cyclase reaction (first requirement for two electrons, followed by removal of four electrons), it may be significant that the flavin moiety of FNR is capable of accepting two electrons (Batie and Kamin, 1986), and that its reduced state is a poor donor of electrons to oxygen (Bes *et al.*, 1995). There are several ways that FNR could support the cyclase reaction. First, if NADPH is the effective electron donor to the reaction, FNR could create an NADPH-rich environment at the cyclase complex. Effective NADPH

concentrations are considered to be surprisingly low in the stroma, with a large proportion bound to proteins such as malate dehydrogenase and ribulose 1,5-bisphosphate carboxylase (Latouche *et al.*, 2000), and therefore local concentration mechanisms might be significant against the background of heavy demand from the Calvin-Benson cycle. Alternatively, FNR could act as a direct electron donor, transferring electrons from photo-reduced Fd to the cyclase reaction. FNR is capable of acting as a diaphorase, and there are reports for FNR reduction of substrates such as methyl viologen (Liochev *et al.*, 1994) and quinones (Bojko *et al.*, 2003).

In both organisms *N. tabacum* and *A. thaliana,* the transgenic lines with a deficit of either FNR1 or YCF54 resulted in MgProtoME accumulation and decreased protein content of either YCF54 in FNR1-deficient lines or FNR1 in YCF54-COS lines (Figures 2, 5, 6). In *A. thaliana* YCF54-COS-lines the Pchlide levels are decreased, whereas they are increased in the *N. tabacum* FNR1-AS lines and the *A. thaliana fnr1* knockout (Figures 2 and 5). In both the tobacco and Arabidopsis plants with disrupted FNR contents the redox state of NADP(H) is more oxidised (Hajirezaei *et al.*, 2002, Kozuleva *et al.*, 2016), resulting in decreased NADPH availability. As the conversion of Pchlide into Chlide by the POR complex is also dependent on NADPH (Heyes and Hunter, 2005), decreased FNR capacity could indirectly cause Pchlide accumulation.

The physiological significance of FNR allocation between the stroma and thylakoid membrane for energy distribution is still a matter of debate. It has been suggested that FNR recruited into the high molecular weight TROL and Tic62 complexes at the thylakoid membrane is not necessary for $NADP^+$ photoreduction (Benz *et al.*, 2010). This has been shown during conditions of active photosynthetic electron transport, when FNR is released from these complexes (Benz *et al.*, 2009, Alte *et al.*, 2010). The sole function suggested to date is that binding to Tic62 and TROL anchors hydrophilic FNR to the thylakoid membrane and chloroplast envelope and stabilizes FNR against degradation (Benz *et al.*, 2009, Juric *et al.*, 2009). But the data presented here offer an alternative explanation. It may be that these tethering proteins function partly to localize FNR in the vicinity of the cyclase complex.

It was previously reported that the redox state of the plastoquinol pool correlated with cyclase activity (Steccanella *et al.,* 2015). The authors proposed that oxidised plastoquinone

could be the electron acceptor from the cyclase reaction, and cyclase activity was impaired in mutants with a higher or excess plastoquinone reduction state. This would fit with the impaired cyclase activity in the tobacco FNR-AS lines, which also have a more reduced PSII acceptor (Hajirezaei *et al.*, 2002), but not with the Arabidopsis *fnr1* mutants, which actually show slightly higher qP values (Lintala *et al.*, 2007, Hanke *et al.*, 2008) corresponding to a more oxidised plastoquinone pool. It therefore seems possible that a complex co-ordination of redox components is necessary for optimal cyclase activity.

It is also worth mentioning that impaired iron sulfur cluster biosynthesis is accompanied by the accumulation of Mg porphyrins and Pchlide, but in particular of MgProtoME (Hu *et al.*, 2017). The authors proposed that cyclase activity is impaired in *SUFB*-deficient mutants, which are affected in the formation of Fe-S clusters. Considering that [2Fe-2S] cluster-containing Fd, the electron donor to FNR, is among the first proteins to decrease in abundance following iron deficiency (Giro *et al.*, 2006, Tognetti *et al.*, 2006), disruption of electron supply to FNR1 as result of a shortage of Fe-S clusters to support the NADPH-dependent cyclase reaction may be part of the explanation for the observed phenotype.

In summary, results obtained in the present study indicate a physiologically relevant interaction between YCF54 and FNR1. A potential role of FNR in electron donation could involve recruitment in order to promote an enriched NADPH micro-environment at the cyclase complex or direct involvement in electron transfer. Further elucidation of a direct FNR involvement in cyclase activity is limited due to the lack of a reliable cyclase assay with either recombinant proteins or green plastids that could be combined with recombinant YCF54, CHL27 and FNR1 to elucidate the mode of this interdependency. Thus, the potential role of YCF54 for connection of the cyclase reaction with active PSI complexes for the electron transfer from FNR1 to the TBS requires further elucidation.

Experimental procedures

Plant material and growth conditions

Seedlings of transgenic, mutant and wild-type *A. thaliana* lines, (YCF54-COS and OEX lines, a FNR1 T-DNA insertion mutant (Hanke *et al.*, 2005, Twachtmann *et al.*, 2012) and FNR1 antisense and sense *N. tabacum* lines (Hajirezaei *et al.*, 2002) were grown for four weeks at

120 µE m^{-2} s^{-1} and 21°C on soil. *A. thaliana* seedlings were grown under short-day conditions (8h light, 16h dark), *N. tabacum* seedlings under long-day conditions (16h light, 8h dark).

Recombinant expression of the YCF54-6xHis protein in *E. coli*

The coding sequence of YCF54 (At5g58250) without the transit peptide was amplified from an *A. thaliana* (Col-0) cDNA library using primers AGGATCCAGCACCAAGTACCATTTC and CGCTCAGCCTATACTGCAGATTCTTGGGTT carrying BamHI and BlpI restriction sites and ligated into the inducible bacterial pET28a(+) expression vector (Novagen®; USA), which was used for chemical transformation of *E. coli* BL21 cells. The expressed YCF54 protein containing a 6x-His-tag was purified by using Ni-NTA columns (QUIAGEN; GER) according to the manufacturer instruction.

Construction of HA-Strep-tagged YCF54 transgenic *A. thaliana* lines

The At5g58250 coding sequence was amplified with the primers TATCGATATGTGGAGCGTCACCG and TCCCGGGTACTGCAGATTCTTGGGTTAC (with adjacent ClaI and XmaI sites) using an *A. thaliana* cDNA library as a template. The obtained 817bp DNA fragment was ligated into the plant binary pXCS-HA-Strep vector (Witte *et al.*, 2004), AY457636). The *YCF54* fragment was linked with the sequences of a 35SCaMV promoter and for a C-terminal HA-Step-tag. The transgenic vector was stably transformed into *A. thaliana* via floral-dip by using the *A. tumefaciens* GV3103 strain. Positive transformants were selected through BASTA® resistance.

Isolation of intact chloroplasts

Four-week-old wild-type *A. thaliana* seedlings were harvested and homogenized in HB buffer (0.45 M sorbitol, 20 mM Tricine-KOH pH 8.4, 10 mM EDTA, 10 mM $NaHCO_3$, 0.1 % (w/v) BSA). The homogenate was filtrated through 2 layers of Miracloth gauze. The received suspension was centrifuged at 500 xg for 8 min, at 4 °C, and the pellet was resuspended in RB buffer (1.5 M sorbitol, 100 mM Tricine-KOH, pH 8.4, 12.5 mM EDTA, 25 mM $MgCl_2$). The suspension was separated over a Percoll gradient. Afterwards chloroplasts were washed once with 1x RB buffer. The pellet was resuspended in lyse buffer (20 mM Tricine-KOH, 2.5 mM EDTA, 5 mM $MgCl_2$, protease inhibitor cocktail (Roche, Switzerland)). Membrane

proteins were solubilized with 0.2 % (w/v) n-dodecyl-β-D-maltoside for 15 min. The supernatant was used for further applications.

Pull-down assay

The purified 6x-His-tagged YCF54 (750 µg) was incubated in 50 % Ni-NTA-Agarose and PBS (150 mM NaCl, 20 mM Na_2HPO_4/NaH_2PO_4, 100mM Tris, 10 % glycerol, 2 % SDS, 100 mM DTT, 0.1 % Bromophenol blue, pH 6.8) containing protease inhibitor cocktail (Roche; CHE), for 1 h at 4 °C, prior to incubation of bound YCF54 with solubilized chloroplasts for 1 h at 4 °C, transfer to a filter column (QIAGEN, Germany). After several washing steps, bound proteins were relieved from the matrix with elution buffer (50 mM NaH_2PO_4, 300 mM NaCl; 250 mM Imidazole, pH 8.0).

Protein gel electrophoresis and immuno-blotting

Protein extracts of leaves, chloroplasts or pull-down eluates were separated by 12% SDS-PAGE, followed by transfer to a nitrocellulose membrane. Membranes were incubated with specific antibody. The chemiluminescence signal from Clarity™ Western ECL Blotting Substrate (Bio-Rad) was detected by Stella 3200 (raytest, Germany).

Extraction of porphyrins and pigments and HPLC analysis

Homogenized leaf material was dissolved in basic acetone (acetone: 0.1 M NH_4OH (9:1, v/v)). To avoid porphyrin degradation, all steps were performed in dim or green safety light. The samples were incubated at -20°C for 20 min, centrifuged at 17,982xg for 10 min, at 4°C. For the analysis, a HPLC device (Agilent, Germany) was used as previously described (Kim et al., 2013; Richter et al., 2013). Identification and quantification were performed using known standards for all analysed Chl and Chl metabolites.

ALA synthesis capacity

As previously described (Mauzerall and Granick, 1956), leaf discs were incubated in 20 mM potassium phosphate buffer (pH 7.2) containing 40 mM levulinic acid for 4 h under standard light intensities, harvested, homogenized and resuspended in 1 ml potassium phosphate buffer. After centrifugation (20 min; 13,000 rpm) the supernatant was mixed with one-quarter Vol of ethyl acetoacetate and heated for 10 min at 95°C. Subsequently, the samples were chilled on ice for 3 min and mixed with 1 Vol modified Ehrlich's reagent (75% (v/v) glacial acetic acid; 12.5 % (v/v) perchloric acid; 3.1 g/l mercury (II) chloride, 0.018 g/l para-dimethylaminobenzaldehyde). The concentration of ALA was spectrophotometrically determined and compared to ALA standards.

77 K Chl a fluorescence emission

Leaf material was homogenized in LHC buffer (50 mM Tricine; 0.4 M sorbitol, pH 7.8) according to Krupa *et al.* (1987), mixed 1:1 with 80 % glycerol, filled up in a capillary and frozen in liquid nitrogen. Chl a fluorescence was determined (λex 440nm, λem 650-680 nm) with a fluorescence spectrophotometer (Hitachi F-7000).

Bimolecular fluorescence complementation (BiFC) assay

The genomic sequences without transit peptide of CHL27 and YCF54 (provided Maxi Rothbart, Plant Physiology, Humboldt-University Berlin) and FNR1 were cloned into the two destination vectors pDEST-GW-VYNE (G1) and pDEST-GW-VYCE (G3) via the GATEWAY® technology (Gehl *et al.*, 2009). These vectors contain either the N-terminal (G1) or C-terminal (G3) fragment of the yellow fluorescence protein Venus. The vectors were introduced into *A. tumefaciens* GV2260, which were co-infiltrated into *N. benthamian*a leaves. After 3 days in darkness, the infiltrated leaf areas were analyzed with the confocal microscope (Leica TCS SP2, GER). Interaction of both fusion-proteins was detected by yellow fluorescence (λex 514 nm, λem 525–600 nm). Chl auto-fluorescence was detected at λex 620–700 nm

Quantitative RT-PCR

For each gene, leaf samples of three plants were pooled for RNA isolation by using the TRIzol reagent (Life Technology, USA). One µg RNA was treated with DNase (NEB; UK) and used for cDNA synthesis (Revert Aid Transcriptase; Thermo Scientific; Germany). The SensimixTM SYBR NO-ROX Kit (Bioline; Germany) was used for qRT-PCR. Analyses were performed using a CFX 96 real-time system (Bio-Rad) device. The used primer pairs for each transcript were given in the Supplemental Table. The transcript levels were normalized to GADPH3 expression and compared with their wild-type expression level.

Thylakoid extraction and BN- PAGE

Five-week-old plants were harvested. Leaf material was ground in HB buffer (0.45 M sorbitol, 20 mM Tricine-KOH pH 8.4, 10 mM EDTA, 10 mM NaHCO3, 0.1 % (w/v) BSA) and filtrated through two layers of Miracloth gauze. The homogenate was centrifuged for 4 min at 5,000 xg and 4°C. The pellet was washed twice with washing buffer (10 mM Tricine, 10 mM NaCl, 10 mM $MgCl_2$). The final pellet was resuspended in BTH buffer (25 % (w/v) bis-tris, 30 % (v/v) glycerol) and stored at -80 °C. The Chl concentration of extracted thylakoids were adjusted to 0.5 µg/µl Chl. Thylakoids for were solubilized with 1 % (w/v) n-dodecyl-β-D-maltoside for 5 min on ice. BN-PAGE analysis were performed as described earlier (Peng et al., 2008)

Acknowledgements

The generous gift of FNR1 antisense and sense *N. tabacum* lines by Prof. Uwe Sonnewald, Friedrich-Alexander-University Erlangen-Nuremberg is acknowledged. The work was supported by a grant from the Deutsche Forschungsgemeinschaft (DFG 936 16-1, Research Unit 2092, Biogenesis of thylakoid membranes) given to BG. The authors declare no conflict of interest.

Supporting Information Legend

Supporting Table S1. Used primers for qRTPCR analysis.

References

Alawady, A.E. and Grimm, B. (2005) Tobacco Mg protoporphyrin IX methyltransferase is involved in inverse activation of Mg porphyrin and protoheme synthesis. *The Plant J*, **41**, 282-290.

Albus, C.A., Salinas, A., Czarnecki, O., Kahlau, S., Rothbart, M., Thiele, W., Lein, W., Bock, R., Grimm, B. and Schottler, M.A. (2012) LCAA, a novel factor required for Mg protoporphyrin monomethylester cyclase accumulation and feedback-control of aminolevulinic acid biosynthesis in tobacco. *Plant Physiol*, **160,** 1923-39

Alcantara-Sanchez, F., Leyva-Castillo, L.E., Chagolla-Lopez, A., Gonzalez de la Vara, L. and Gomez-Lojero, C. (2017) Distribution of isoforms of ferredoxin-NADP+ reductase (FNR) in cyanobacteria in two growth conditions. *The Int J Biochem Cell Biol*, **85**, 123-134.

Alte, F., Stengel, A., Benz, J.P., Petersen, E., Soll, J., Groll, M. and Bolter, B. (2010) Ferredoxin:NADPH oxidoreductase is recruited to thylakoids by binding to a polyproline type II helix in a pH-dependent manner. *Proc Natl Acad Sci U S A*, **107**, 19260-19265.

Anderson, J.M., Palukaitis, P. and Zaitlin, M. (1992) A defective replicase gene induces resistance to cucumber mosaic virus in transgenic tobacco plants. *Proc Natl Acad Sci U S A*, **89**, 8759-8763.

Batie, C.J. and Kamin, H. (1986) Association of ferredoxin-NADP+ reductase with NADP(H) specificity and oxidation-reduction properties. *J Biol Chem*, **261**, 11214-11223.

Benz, J.P., Lintala, M., Soll, J., Mulo, P. and Bolter, B. (2010) A new concept for ferredoxin-NADP(H) oxidoreductase binding to plant thylakoids. *Trends in Plant Science*, **15**, 608-613.

Benz, J.P., Stengel, A., Lintala, M., Lee, Y.H., Weber, A., Philippar, K., Gugel, I.L., Kaieda, S., Ikegami, T., Mulo, P., Soll, J. and Bolter, B. (2009) Arabidopsis Tic62 and ferredoxin-NADP(H) oxidoreductase form light-regulated complexes that are integrated into the chloroplast redox poise. *Plant Cell*, **21**, 3965-3983.

Berthold, D.A. and Stenmark, P. (2003) Membrane-bound diiron carboxylate proteins. *Annu Rev Plant Biol*, **54**, 497-517.

Bes, M.T., De Lacey, A.L., Peleato, M.L., Fernandez, V.M. and Gomez-Moreno, C. (1995) The covalent linkage of a viologen to a flavoprotein reductase transforms it into an oxidase. *Eur J Biochem*, **233**, 593-599.

Bojko, M., Kruk, J. and Wieckowski, S. (2003) Plastoquinones are effectively reduced by ferredoxin:NADP+ oxidoreductase in the presence of sodium cholate micelles. Significance for cyclic electron transport and chlororespiration. *Phytochem*, **64**, 1055-1060.

Bollivar, D., Braumann, I., Berendt, K., Gough, S.P. and Hansson, M. (2014) The Ycf54 protein is part of the membrane component of Mg-protoporphyrin IX monomethyl ester cyclase from barley (Hordeum vulgare L.). *The FEBS J*, **281**, 2377-2386.

Bollivar, D.W. and Beale, S.I. (1995) Formation of the isocyclic ring of chlorophyll by isolated Chlamydomonas reinhardtii chloroplasts. *Photosyn Res*, **43**, 113-124.

Brzezowski, P., Richter, A.S. and Grimm, B. (2015) Regulation and function of tetrapyrrole biosynthesis in plants and algae. *Biochim Biophys Acta*, **1847**, 968-985.

Clark, R.D., Hawkesford, M.J., Coughlan, S.J., Bennett, J. and Hind, G. (1984) Association of Ferredoxin-Nadp+ Oxidoreductase with the Chloroplast Cytochrome B-F Complex. *Febs Lett*, **174**, 137-142.

Gehl, C., Waadt, R., Kudla, J., Mendel, R.R. and Hansch, R. (2009) New GATEWAY vectors for high throughput analyses of protein-protein interactions by bimolecular fluorescence complementation. *Mol Plant*, **2**, 1051-1058.

Giro, M., Carrillo, N. and Krapp, A.R. (2006) Glucose-6-phosphate dehydrogenase and ferredoxin-NADP(H) reductase contribute to damage repair during the soxRS response of Escherichia coli. *Microbiology*, **152**, 1119-1128.

Guedeney, G., Corneille, S., Cuine, S. and Peltier, G. (1996) Evidence for an association of ndh B, ndh J gene products and ferredoxin-NADP-reductase as components of a chloroplastic NAD(P)H dehydrogenase complex. *FEBS Lett*, **378**, 277-280.

Hajirezaei, M.R., Peisker, M., Tschiersch, H., Palatnik, J.F., Valle, E.M., Carrillo, N. and Sonnewald, U. (2002) Small changes in the activity of chloroplastic NADP(+)-dependent ferredoxin oxidoreductase lead to impaired plant growth and restrict photosynthetic activity of transgenic tobacco plants. *The Plant J*, **29**, 281-293.

Hanke, G.T., Endo, T., Satoh, F. and Hase, T. (2008) Altered photosynthetic electron channelling into cyclic electron flow and nitrite assimilation in a mutant of ferredoxin:NADP(H) reductase. *Plant Cell Env*, **31**, 1017-1028.

Hanke, G.T., Okutani, S., Satomi, Y., Takao, T., Suzuki, A. and Hase, T. (2005) Multiple iso-proteins of FNR in Arabidopsis: evidence for different contributions to chloroplast function and nitrogen assimilation. *Plant Cell Env*, **28**, 1146-1157.

Hey, D., Rothbart, M., Herbst, J., Wang, P., Muller, J., Wittmann, D., Gruhl, K. and Grimm, B. (2017) LIL3, a light-harvesting complex protein, links terpenoid and tetrapyrrole biosynthesis. *Plant Physiol*, **174**, 1037-1050

Heyes, D.J. and Hunter, C.N. (2005) Making light work of enzyme catalysis: protochlorophyllide oxidoreductase. *Trends in biochemical sciences*, **30**, 642-649.

Hollingshead, S., Bliss, S., Baker, P.J. and Neil Hunter, C. (2017) Conserved residues in Ycf54 are required for protochlorophyllide formation in Synechocystis sp. PCC 6803. *The Biochem J*, **474**, 667-681.

Hollingshead, S., Kopecna, J., Armstrong, D.R., Bucinska, L., Jackson, P.J., Chen, G.E., Dickman, M.J., Williamson, M.P., Sobotka, R. and Hunter, C.N. (2016) Synthesis of Chlorophyll-Binding Proteins in a Fully Segregated Deltaycf54 Strain of the Cyanobacterium Synechocystis PCC 6803. *Front Plant Sci*, **7**, 292.

Hollingshead, S., Kopecna, J., Jackson, P.J., Canniffe, D.P., Davison, P.A., Dickman, M.J., Sobotka, R. and Hunter, C.N. (2012) Conserved chloroplast open-reading frame ycf54 is required for activity of the magnesium protoporphyrin monomethylester oxidative cyclase in Synechocystis PCC 6803. *J Biol Chem*, **287**, 27823-27833.

Hu, X., Page, M.T., Sumida, A., Tanaka, A., Terry, M.J. and Tanaka, R. (2017) The iron-sulfur cluster biosynthesis protein SUFB is required for chlorophyll synthesis, but not phytochrome signaling. *The Plant journal : for cell and molecular biology*, **89**, 1184-1194.

Joliot, P. and Johnson, G.N. (2011) Regulation of cyclic and linear electron flow in higher plants. *P Natl Acad Sci U S A*, **108**, 13317-13322.

Juric, S., Hazler-Pilepic, K., Tomasic, A., Lepedus, H., Jelicic, B., Puthiyaveetil, S., Bionda, T., Vojta, L., Allen, J.F., Schleiff, E. and Fulgosi, H. (2009) Tethering of ferredoxin:NADP+ oxidoreductase to thylakoid membranes is mediated by novel chloroplast protein TROL. *The Plant J*, **60**, 783-794.

Kauss, D., Bischof, S., Steiner, S., Apel, K. and Meskauskiene, R. (2012) FLU, a negative feedback regulator of tetrapyrrole biosynthesis, is physically linked to the final steps of the Mg(++)-branch of this pathway. *FEBS Lett*, **586**, 211-216.

Kim, S., Schlicke, H., Van Ree, K., Karvonen, K., Subramaniam, A., Richter, A., Grimm, B. and Braam, J. (2013) Arabidopsis chlorophyll biosynthesis: an essential balance between the methylerythritol phosphate and tetrapyrrole pathways. *Plant Cell*, **25**, 4984-4993.

Komenda, J., Sobotka, R. and Nixon, P.J. (2012) Assembling and maintaining the Photosystem II complex in chloroplasts and cyanobacteria. *Curr Opin Plant Biol*, **15**, 245-251.

Korn, A., Ajlani, G., Lagoutte, B., Gall, A. and Setif, P. (2009) Ferredoxin:NADP+ oxidoreductase association with phycocyanin modulates its properties. *J Biol Chem*, **284**, 31789-31797.

Kozuleva, M., Goss, T., Twachtmann, M., Rudi, K., Trapka, J., Selinski, J., Ivanov, B., Garapati, P., Steinhoff, H.J., Hase, T., Scheibe, R., Klare, J.P. and Hanke, G.T. (2016) Ferredoxin:NADP(H) Oxidoreductase Abundance and Location Influences Redox Poise and Stress Tolerance. *Plant Physiol*, **172**, 1480-1493.

Krupa, Z., Huner, N.P., Williams, J.P., Maissan, E. and James, D.R. (1987) Development at Cold-Hardening Temperatures : The Structure and Composition of Purified Rye Light Harvesting Complex II. *Plant Physiol*, **84**, 19-24.

Latouche, G., Cerovic, Z.G., Montagnini, F. and Moya, I. (2000) Light-induced changes of NADPH fluorescence in isolated chloroplasts: a spectral and fluorescence lifetime study. *Biochim Biophys Acta*, **1460**, 311-329.

Lintala, M., Allahverdiyeva, Y., Kangasjarvi, S., Lehtimaki, N., Keranen, M., Rintamaki, E., Aro, E.M. and Mulo, P. (2009) Comparative analysis of leaf-type ferredoxin-NADP(+) oxidoreductase isoforms in Arabidopsis thaliana. *The Plant J*, **57**, 1103-1115.

Lintala, M., Allahverdiyeva, Y., Kidron, H., Piippo, M., Battchikova, N., Suorsa, M., Rintamaki, E., Salminen, T.A., Aro, E.M. and Mulo, P. (2007) Structural and functional characterization of ferredoxin-NADP+-oxidoreductase using knock-out mutants of Arabidopsis. *The Plant J*, **49**, 1041-1052.

Lintala, M., Lehtimaki, N., Benz, J.P., Jungfer, A., Soll, J., Aro, E.M., Bolter, B. and Mulo, P. (2012) Depletion of leaf-type ferredoxin-NADP(+) oxidoreductase results in the permanent induction of photoprotective mechanisms in Arabidopsis chloroplasts. *The Plant J*, **70**, 809-817.

Liochev, S.I., Hausladen, A., Beyer, W.F., Jr. and Fridovich, I. (1994) NADPH: ferredoxin oxidoreductase acts as a paraquat diaphorase and is a member of the soxRS regulon. *Proc Natl Acad Sci U S A*, **91**, 1328-1331.

Mauzerall, D. and Granick, S. (1956) The occurrence and determination of delta-amino-levulinic acid and porphobilinogen in urine. *J Biol Chem*, **219**, 435-446.

Minamizaki, K., Mizoguchi, T., Goto, T., Tamiaki, H. and Fujita, Y. (2008) Identification of two homologous genes, chlAI and chlAII, that are differentially involved in isocyclic ring formation of chlorophyll a in the cyanobacterium Synechocystis sp. PCC 6803. *J Biol Chem*, **283**, 2684-2692.

Moseley, J.L., Page, M.D., Alder, N.P., Eriksson, M., Quinn, J., Soto, F., Theg, S.M., Hippler, M. and Merchant, S. (2002) Reciprocal expression of two candidate di-iron enzymes affecting photosystem I and light-harvesting complex accumulation. *Plant Cell*, **14**, 673-688.

Nordlund, P. and Eklund, H. (1995) Di-iron-carboxylate proteins. *Current Opinion Struct Biol*, **5**, 758-766.

Okutani, S., Hanke, G.T., Satomi, Y., Takao, T., Kurisu, G., Suzuki, A. and Hase, T. (2005) Three maize leaf ferredoxin:NADPH oxidoreductases vary in subchloroplast location, expression, and interaction with ferredoxin. *Plant Physiol*, **139**, 1451-1459.

Ouchane, S., Steunou, A.S., Picaud, M. and Astier, C. (2004) Aerobic and anaerobic Mg-protoporphyrin monomethyl ester cyclases in purple bacteria: a strategy adopted to bypass the repressive oxygen control system. *J Biol Chem*, **279**, 6385-6394.

Papenbrock, J., Pfundel, E., Mock, H.P. and Grimm, B. (2000) Decreased and increased expression of the subunit CHL I diminishes Mg chelatase activity and reduces chlorophyll synthesis in transgenic tobacco plants. *The Plant J,* **22**, 155-164.

Peng, L., Shimizu, H. and Shikanai, T. (2008**)** The chloroplast NAD(P)H dehydrogenase complex interacts with photosystem I in Arabidopsis. *J Biol Chem* **283**, 34873-34879

Peter, E., Salinas, A., Wallner, T., Jeske, D., Dienst, D., Wilde, A. and Grimm, B. (2009) Differential requirement of two homologous proteins encoded by sll1214 and sll1874 for the reaction of Mg protoporphyrin monomethylester oxidative cyclase under aerobic and micro-oxic growth conditions. *Biochim Biophys Acta*, **1787**, 1458-1467.

Pinta, V., Picaud, M., Reiss-Husson, F. and Astier, C. (2002) Rubrivivax gelatinosus acsF (previously orf358) codes for a conserved, putative binuclear-iron-cluster-containing protein involved in aerobic oxidative cyclization of Mg-protoporphyrin IX monomethylester. *J Bacteriol*, **184**, 746-753.

Porra, R.J., Schafer, W., Gad'on, N., Katheder, I., Drews, G. and Scheer, H. (1996) Origin of the two carbonyl oxygens of bacteriochlorophyll a. Demonstration of two different pathways for the formation of ring E in Rhodobacter sphaeroides and Roseobacter denitrificans, and a common hydratase mechanism for 3-acetyl group formation. *Eur J Biochem*, **239**, 85-92.

Porra, R.J., Urzinger, M., Winkler, J., Bubenzer, C. and Scheer, H. (1998) Biosynthesis of the 3-acetyl and 13(1)-oxo groups of bacteriochlorophyll a in the facultative aerobic bacterium, Rhodovulum sulfidophilum--the presence of both oxygenase and hydratase pathways for isocyclic ring formation. *Eur J Biochem*, **257**, 185-191.

Richter, A.S., Peter, E., Rothbart, M., Schlicke, H., Toivola, J., Rintamaki, E. and Grimm, B. (2013) Posttranslational Influence of NADPH-Dependent Thioredoxin Reductase C on Enzymes in Tetrapyrrole Synthesis. *Plant Physiol*, **162**, 63-73.

Rodriguez, R.E., Lodeyro, A., Poli, H.O., Zurbriggen, M., Peisker, M., Palatnik, J.F., Tognetti, V.B., Tschiersch, H., Hajirezaei, M.R., Valle, E.M. and Carrillo, N. (2007) Transgenic tobacco plants overexpressing chloroplastic ferredoxin-NADP(H) reductase display normal rates of photosynthesis and increased tolerance to oxidative stress. *Plant Physiol*, **143**, 639-649.

Rzeznicka, K., Walker, C.J., Westergren, T., Kannangara, C.G., von Wettstein, D., Merchant, S., Gough, S.P. and Hansson, M. (2005) Xantha-l encodes a membrane subunit of the aerobic Mg-protoporphyrin IX monomethyl ester cyclase involved in chlorophyll biosynthesis. *Proc Natl Acad Sci U S A*, **102**, 5886-5891.

Shalygo, N., Czarnecki, O., Peter, E. and Grimm, B. (2009) Expression of chlorophyll synthase is also involved in feedback-control of chlorophyll biosynthesis. *Plant Mol Biol,* 71, 425-36.

Sobotka, R. (2014) Making proteins green; biosynthesis of chlorophyll-binding proteins in cyanobacteria. *Photosyn Res*, **119**, 223-232.

Steccanella, V., Hansson, M. and Jensen, P.E. (2015) Linking chlorophyll biosynthesis to a dynamic plastoquinone pool. *Plant Physiol Biochem*, **97**, 207-216.

Stenbaek, A., Hansson, A., Wulff, R.P., Hansson, M., Dietz, K.J. and Jensen, P.E. (2008) NADPH-dependent thioredoxin reductase and 2-Cys peroxiredoxins are needed for the protection of Mg-protoporphyrin monomethyl ester cyclase. *FEBS Lett*, **582**, 2773-2778.

Tanaka, A., Ito, H., Tanaka, R., Tanaka, N.K., Yoshida, K. and Okada, K. (1998) Chlorophyll a oxygenase (CAO) is involved in chlorophyll b formation from chlorophyll a. *Proc Natl Acad Sci U S A*, **95**, 12719-12723.

Tanaka, R., Oster, U., Kruse, E., Rudiger, W. and Grimm, B. (1999) Reduced activity of geranylgeranyl reductase leads to loss of chlorophyll and tocopherol and to partially geranylgeranylated chlorophyll in transgenic tobacco plants expressing antisense RNA for geranylgeranyl reductase. *Plant Physiol*, **120**, 695-704.

Tanaka, R., Rothbart, M., Oka, S., Takabayashi, A., Takahashi, K., Shibata, M., Myouga, F., Motohashi, R., Shinozaki, K., Grimm, B. and Tanaka, A. (2010) LIL3, a light-harvesting-like protein, plays an essential role in chlorophyll and tocopherol biosynthesis. *Proc Natl Acad Sci U S A*, **107**, 16721-16725.

Tanaka, R. and Tanaka, A. (2007) Tetrapyrrole biosynthesis in higher plants. *Annu Rev Plant Biol*, **58**, 321-346.

Tanaka, R. and Tanaka, A. (2011) Chlorophyll cycle regulates the construction and destruction of the light-harvesting complexes. *Biochim Biophys Acta*, **1807**, 968-976.

Thomas, J.C., Ughy, B., Lagoutte, B. and Ajlani, G. (2006) A second isoform of the ferredoxin : NADP oxidoreductase generated by an in-frame initiation of translation. *Proc Natl Acad Sci U S A*, **103**, 18368-18373.

Tognetti, V.B., Palatnik, J.F., Fillat, M.F., Melzer, M., Hajirezaei, M.R., Valle, E.M. and Carrillo, N. (2006) Functional replacement of ferredoxin by a cyanobacterial flavodoxin in tobacco confers broad-range stress tolerance. *Plant Cell*, **18**, 2035-2050.

Tottey, S., Block, M.A., Allen, M., Westergren, T., Albrieux, C., Scheller, H.V., Merchant, S. and Jensen, P.E. (2003) Arabidopsis CHL27, located in both envelope and thylakoid membranes, is required for the synthesis of protochlorophyllide. *Proc Natl Acad Sci U S A*, **100**, 16119-16124.

Twachtmann, M., Altmann, B., Muraki, N., Voss, I., Okutani, S., Kurisu, G., Hase, T. and Hanke, G.T. (2012) N-terminal structure of maize ferredoxin:NADP+ reductase determines recruitment into different thylakoid membrane complexes. *Plant Cell*, **24**, 2979-2991.

Walker, C.J., Castelfranco, P.A. and Whyte, B.J. (1991) Synthesis of divinyl protochlorophyllide. Enzymological properties of the Mg-protoporphyrin IX monomethyl ester oxidative cyclase system. *The Biochem J*, **276** , 691-697.

Wang, P. and Grimm, B. (2015) Organization of chlorophyll biosynthesis and insertion of chlorophyll into the chlorophyll-binding proteins in chloroplasts. *Photosynth Res*. **126**, 189-202

Witte, C.P., Noel, L.D., Gielbert, J., Parker, J.E. and Romeis, T. (2004) Rapid one-step protein purification from plant material using the eight-amino acid StrepII epitope. *Plant Mol Biol*, **55**, 135-147.

Wong, Y.S. and Castelfranco, P.A. (1984) Resolution and Reconstitution of Mg-Protoporphyrin IX Monomethyl Ester (Oxidative) Cyclase, the Enzyme System Responsible for the Formation of the Chlorophyll Isocyclic Ring. *Plant Physiol*, **75**, 658-661.

Zhang, H., Whitelegge, J.P. and Cramer, W.A. (2001) Ferredoxin:NADP+ oxidoreductase is a subunit of the chloroplast cytochrome b6f complex. *J Biol Chem*, **276**, 38159-38165.

Figure Legends

Figure 1. Loss of YCF54 leads to a chlorotic phenotype and altered protein levels of *A. thaliana* seedlings. (A) Phenotype of lines with modified *YCF54* expression (YCF54-COS, co-suppression of YCF54, YCF54-OEX, over-expression of YCF54 containing a HA-Strep-tag are presented in comparison to wild type (Col-0). Plants were grown for four weeks under short day conditions (8h light, 16h dark), 120 µE m^{-2} s^{-1} and 21°C. (B) Western blot analysis for YCF54 and CHL27. Equal protein amounts of leaf extracts from two representative COS and OEX lines were loaded on a 12% SDS gel. The YCF54-antibody detects both endogenous and transgenic YCF54. (C) Relative expression of endogenous *YCF54* (*YCF54 UTR*) and total *YCF54,* as well as *CHL27* determined by qRT-PCR analysis and normalized as relative values to *GAPDH* and to expression in wild-type (ΔΔCt). (D) Chl a/b analysis by HPLC and (E) Chl a/b ratio in leaf extracts from wild-type, YCF54-COS and OEX lines. Analysis of endogenous *YCF54* RNA content was performed by using a fwd primer, which is specific for the 5'UTR of *YCF54*. In contrast to the endogenous *YCF54* copy, the transgene did not contain this 5'UTR.

(* = p < 0.05; ** = p < 0.01; *** = p < 0,001.) Furthermore, for all following statistics, bars were included to show, which samples were compared pairwise.

Figure 2. Measurement of the contents of tetrapyrrole intermediates indicates strong impairments of the YCF54-COS lines in comparison to YCF54-OEX and control lines. The analyzed amounts are relative to fresh weight (FW) of the leaf samples. For each line four biological replicates were analyzed. (A) Mg protoporphyrin (MgProto) and Mg protoporphyrin monomethylester (MgProtoME), (B) protochlorophyllide (Pchlide) and (C) chlorophyllide (Chlide) contents were determined via HPLC. n.d., not detectable. (D) ALA synthesis capacity was examined by analyzing the amount of ALA, which accumulated in leaf discs after 4-h incubation with levulinic acid. (* = p < 0.05; ** = p < 0.01; *** = p < 0,001).

Figure 3. Composition of photosynthetic protein complexes of a representative YCF54-COS line with reduced YCF54 content and the *chl27* knock-down mutant in comparison to wild type. (A) Immune-reactive protein bands for LHCA1, PsaD, PsbA and LHCB1 after separation of protein extracts from wild type and two individual transgenic lines for YCF54-COS and YCF54-OEX (as displayed in Figure 1) on a 12 % SDS PAGE. (B) Protein complexes of isolated thylakoid membranes normalized to identical Chl content were separated on a BN 4–12 % polyacrylamide gel. PSII-LHCII sc, PSII supercomplexes (sc) consisting of core complexes (C) and LHCII trimers bound with moderate (M) and strong (S) affinity. (C) 77K Chl emission spectra. The maximal Chl fluorescence at 686 nm, which represents the PSII-LHCII complexes, was normalized to 1 for each line.

Figure 4. Interaction analysis of cyclase subunits with FNR1. (A) Pull-down assays with recombinant 6xHis-tagged YCF54 as bait, which was immobilized on Ni-NTA agarose, and solubilized wild-type chloroplasts as prey. Eluted proteins were separated by SDS-PAGE, transferred onto a membrane and probed with specific antibodies against FNR1 and CHL27. As negative control, an eluate of an empty matrix as bait and isolated chloroplasts as prey was used to confirm the specific interaction. (B) Bimolecular fluorescence complementation assay for FNR1 interaction with YCF54 and CHL27. The proteins were fused to the N- (G1) and C-terminal halves (G3) of splitYFP and transiently expressed in *N. benthamiana* leaves. The signals in the left panel correspond to the fluorescence (λex at 514 nm) of the

completed Venus protein, Chl auto-fluorescence in the middle panel. The right panel shows the overlay of both Chl and Venus fluorescence, scale bar indicates 10 µm.

Figure 5. Biochemical analysis of *A. thaliana fnr1* knockdown mutant in comparison to YCF54-COS and YCF54-OEX lines. Immunoblot analysis of proteins in wild type (Col-0), *fnr1* and YCF54-COS plants (A) as well as in Col-0 and YCF54-OEX (B) by using antibodies against CHL27, FNR1 and YCF54. Equal amounts of protein were separated on a 12% SDS PAGE. The large subunit of RuBisCO (RBCL) was used as loading control. The impact of *YCF54* expression is shown with two independent YCF54-OEX lines. Analysis of TBS intermediates (as in Figure 2) of control (Col-0), a YCF54-COS line and *fnr1*. The content of MgP and MgProtoME (C), Pchlide (D) and Chlide (E) was related to leaf fresh weight (FW).(* = $p < 0.05$; ** = $p < 0.01$; *** = $p < 0.001$).

Figure 6. Analysis of FNR1 antisense (AS) and sense (S) *N. tabacum* plants compared to control plants (SNN). (A) Young FNR1-AS leaves were pale-green under standard growth conditions, whereas older leaves from FNR1-AS and FNR1-S lines showed wild-type (SNN)-like pigmentation. (B) Immunoblot analysis for cyclase subunits (CHL27 and YCF54) and FNR1 of protein extracts from SNN, three FNR1-AS lines with gradually decreased *FNR1* expression and two FNR1-S lines. Equal protein amounts were separated on 12 % SDS gels. (C-E) HPLC analysis of the Chl content (C) (* = $p < 0.05$), of MgP and MgProtoME (D) and Pchlide (E). The data were related to leaf fresh-weight (FW). n.d. not detectable, (** = $p < 0.01$; *** = $p < 0.001$).

Figure 1

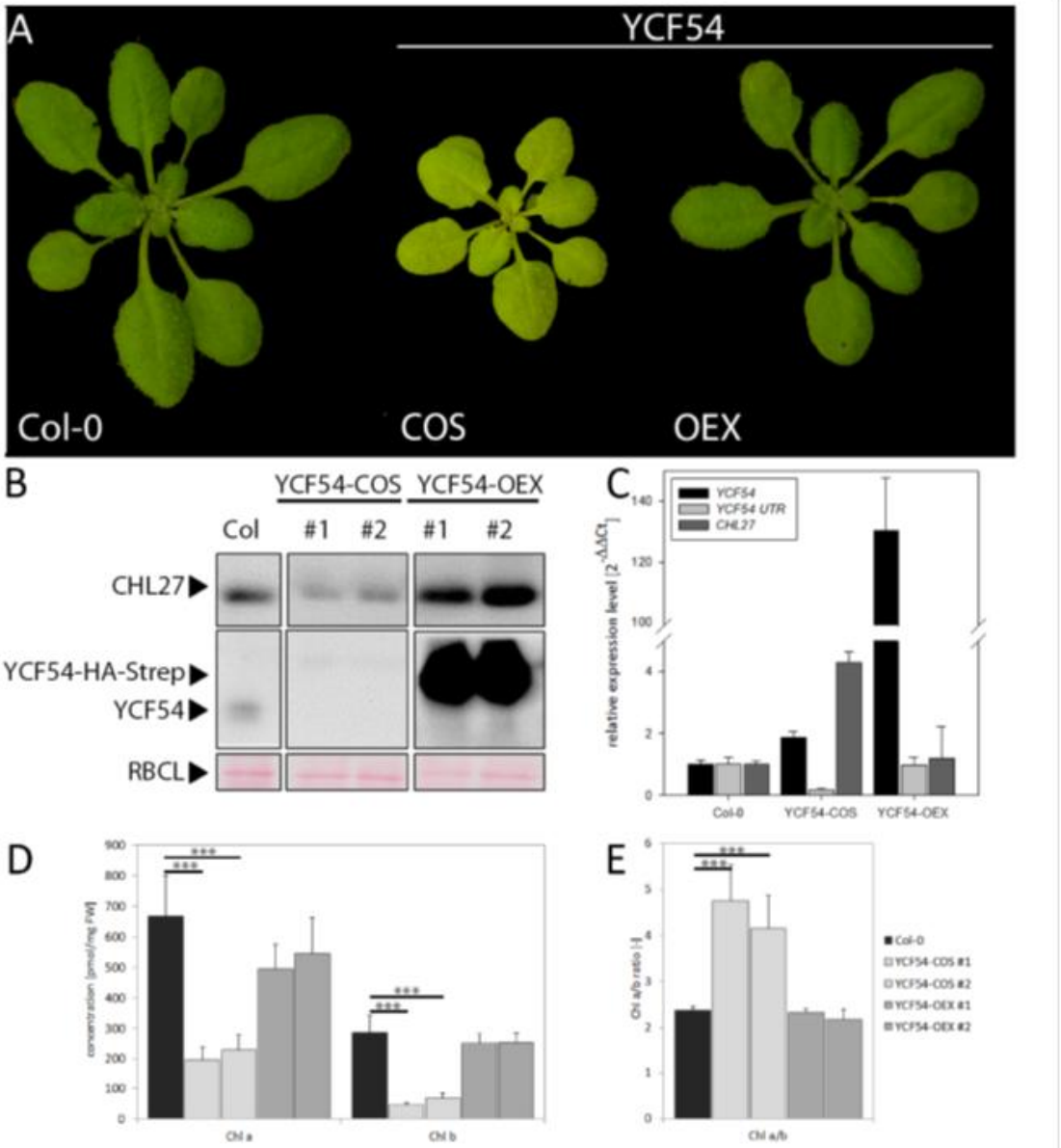

Figure 2

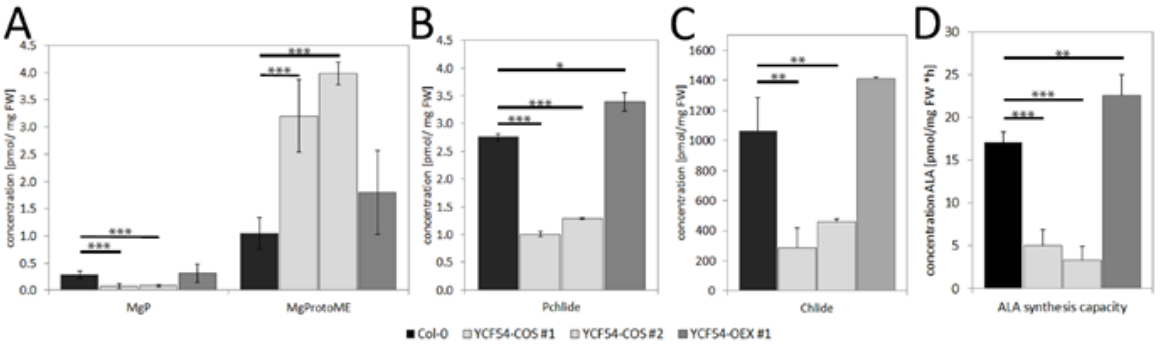

Figure 3

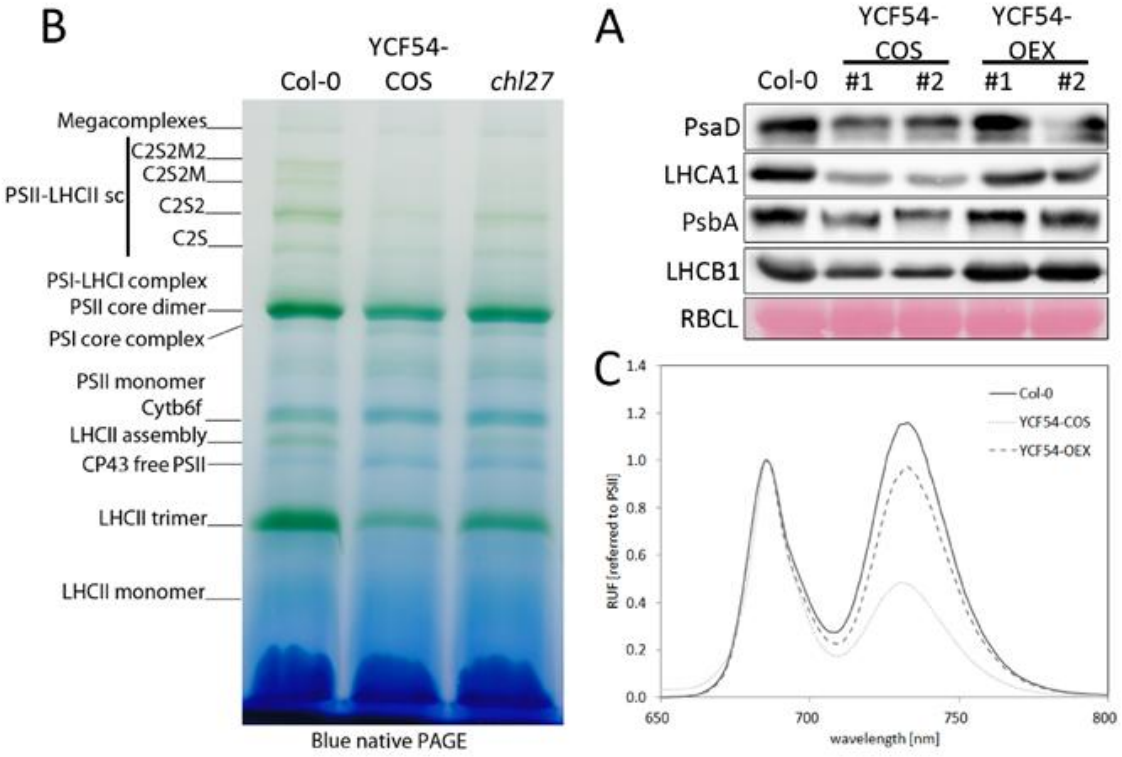

Figure 4

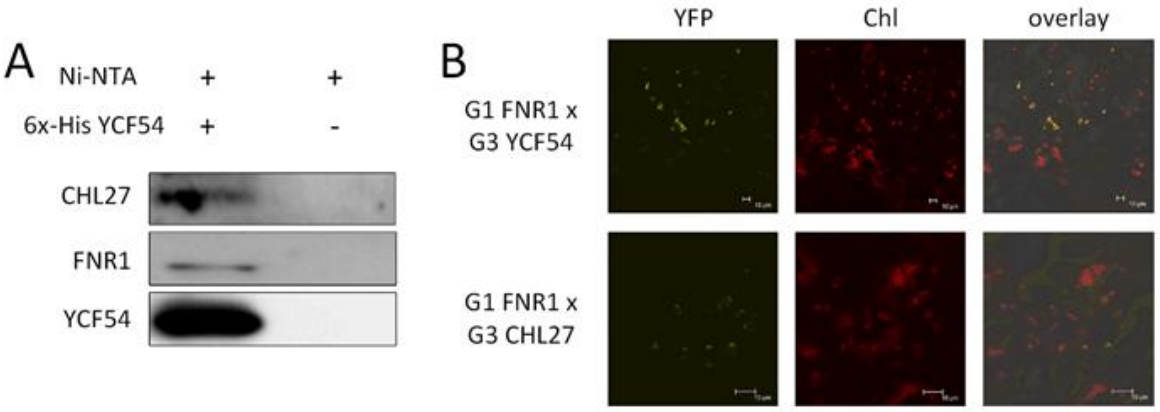

Figure 5

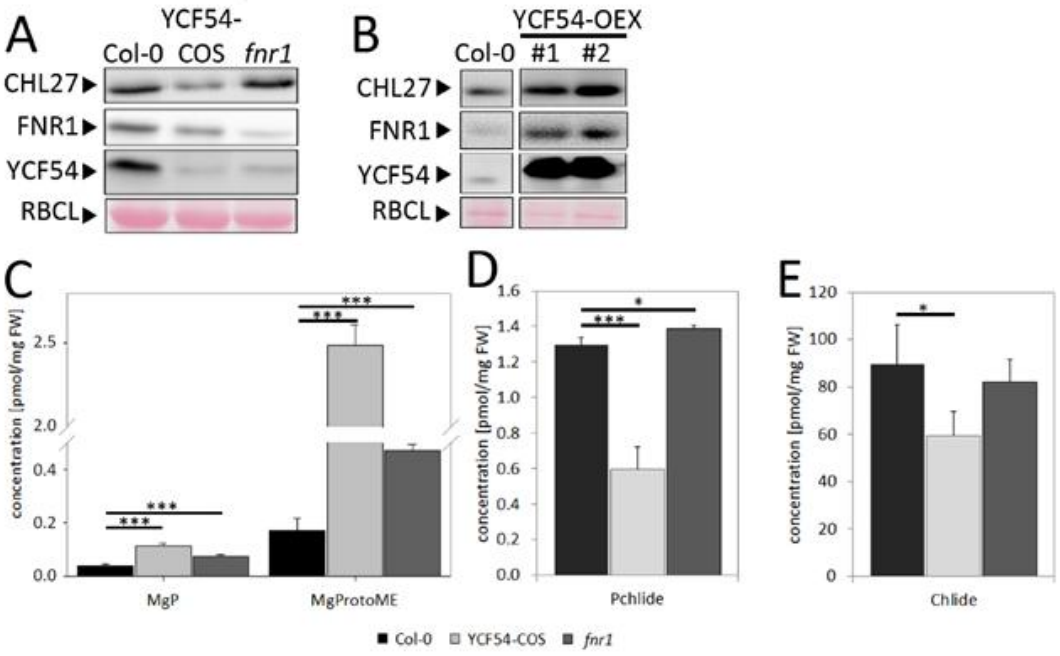

Figure 6